

Comparison of theoretical radiation-driven winds from stars and discs.

Daniel Proga

Imperial College of Science, Technology and Medicine, Blackett Laboratory, Prince Consort Road, London SW7 2BZ, UK
E-mail: d.proga@ic.ac.uk

17 July 2018

ABSTRACT

We compare models of line-driven winds from accretion discs and single spherical stars. We look at the problem of scaling mass-loss rates and velocities of stellar and disc winds with model parameters. We find that stellar and disc winds driven by radiation, within the CAK framework, are very similar as far as mass-loss rates and velocities are concerned. Thus we can use analytic results for stellar winds to rescale, in a first order approximation, numerical results for disc winds. We also show how the CAK stellar solutions change when we take into account effects of very low luminosities or line-driving force.

Key words: accretion discs – hydrodynamics – methods: numerical – stars: mass-loss – stars: early-type – galaxies: nuclei

1 INTRODUCTION

Radiation pressure has been long recognised as effective at powering mass-loss from luminous stars. It has been shown that stars with luminosities as low as 0.1 per cent of their Eddington limit can produce a powerful high velocity wind, when the transmission of radiation pressure to a flow via spectral line opacity is included. Studies of stellar winds driven by radiation pressure due to lines began more than two decades ago (Lucy & Solomon 1970; Castor, Abbott & Klein 1975, hereafter CAK). Later theoretical work by Friend & Abbott (1986) and Pauldrach, Puls & Kudritzki (1986; hereafter PPK) modified the CAK method and reproduced well empirically estimated time-averaged mass-loss rates and terminal velocities for main-sequence and evolved OB stars. After these successes of the modified CAK method, increasingly more attention has been paid to the instabilities inherent in the line-driving mechanism (e.g., Owocki, Castor & Rybicki 1988, here after OCR; Puls, Owocki & Fullerton 1993) and multi-dimensional aspects of stellar winds (e.g., Bjorkman & Cassinelli 1993; Owocki, Cranmer & Blondin 1994).

A strong radiation field can also be produced by accretion discs, which are believed to be important and common components in many astrophysical objects, for example, cataclysmic variables (CVs), high mass young stellar objects (YSOs) and AGNs. Many of these objects show evidence of high velocity winds coming from the disk itself (e.g., Drew 1997; Mundt & Ray 1994; Weymann et al. 1991). Small won-

der then, that radiation pressure has been proposed to power mass-loss also from accretion discs.

Despite a deep and quantitative understanding of radiation-driven winds in stars it has not been straightforward to demonstrate that radiation can produce strong and fast winds from discs. The basic difficulty is the intrinsically two-dimensional, axisymmetric nature of disc winds. First studies of disc winds were focused on finding semi-analytic time-independent solutions. Such an approach required some simplifications and assumptions which had an essential influence on the final outcome (e.g., Vitello & Shlosman 1988; Murray et al 1995). Nevertheless these studies illustrated in more detail the basic differences between driving a wind from a stellar photosphere and a disc photosphere. For example, Vitello & Shlosman showed that an increase of the vertical gravity component with height from the disc mid-plane prevents a disc from producing a wind unless the vertical component of the radiation pressure also increases with height.

Numerical treatments of the disc wind problem have proven to be more successful as they allow solving of the multidimensional dynamical equations from first principles. Relatively early work by Icke (1980; 1981) using two-dimensional, time-dependent numerical simulations showed how radiation pressure due to electrons can produce a disc wind. More recently Pereyra, Kallman & Blondin (1997, see also Pereyra 1997) presented numerical calculations of the dimensional structure of line-driven disc winds for CVs.

However their spatial resolution of wind near a disc was too coarse to capture the wind structure in that critical region.

Proga, Stone & Drew (1998, hereafter PSD) developed another numerical treatment of disc winds. PSD have identified the inner and near disc as the important spatial domain and have therefore used a non-uniform (up to 200×200) grid to ensure that the subsonic acceleration zone near the disc surface is well sampled.

PSD explored the impact upon the mass-loss rate and outflow geometry caused by varying the system luminosity and the radiation field geometry. A striking outcome of PSD's study has been the finding that winds driven from, and illuminated solely by, an accretion disc yield complex, unsteady outflow. In this case, time-independent quantities can be determined only after averaging over several flow timescales. On the other hand, if winds are illuminated by radiation dominated by the central star, then the disc yields steady outflow. PSD also found that the mass-loss rate is a strong function of the total luminosity, while the outflow geometry is determined by the geometry of the radiation field. In particular, for high system luminosities, the disc mass-loss rate scales with the effective Eddington luminosity in a way similar to stellar mass loss. As the system luminosity decreases below a critical value (about twice the Eddington limit), the mass-loss rate decreases quickly to zero.

PSD's calculations have been motivated by and designed for the case of winds from CVs. Their findings are in qualitative agreement with the kinematics of CV outflows inferred from spectroscopic observations. In a second paper (Drew, Proga & Stone 1998; hereafter DPS) they considered both the star and the disc as a source of mass. For model parameters suitable for a typical high mass YSO, where the stellar luminosity is ~ 2 orders of magnitude higher than the intrinsic disc luminosity, their radiation-driven wind disc model might explain the extreme mass-loss signatures of these objects. Most recently Oudmaijer et al. (1998) followed DPS and calculated a model for a B star surrounded by an optically thick disc. The resulting wind configuration could match with the wind structure in B[e] stars. In particular, Oudmaijer et al.'s results show that the kinematic properties of the wind might explain the observed spectral features in HD 87643.

In this paper we look at the problem of scaling disc mass-loss rates and terminal velocities with model parameters. We will use results presented by PSD and DPS and use their approach to calculate some new results. Additionally we will review results for stellar winds to compare them with numerical results for disc winds. For that we will calculate some new stellar wind models for a parameter space not explored before. These new stellar calculations are for relatively low luminosities, like those of white dwarfs and/or a very low increase of radiation pressure due to lines as in highly ionized* or low metallicity winds. We would like to

* Abbott & Friend 1989 considered a related problem of the effects of ionizing shocks in a stellar wind on the terminal velocity

Table 1. Ranges of the model parameters which we have explored.

Parameter	Range
c'_s	$1.53 \times 10^{-3} - 1.38 \times 10^{-2}$
α	0.4 – 0.8
M_{max}	1380 – 4400
Γ_D	$0 - 1.21 \times 10^{-2}$
Γ_*	$0 - 1.21 \times 10^{-2}$

point out that we treat our comparison between models of stellar and disc winds quite formally as our goal is to identify what and how model parameters control the mass-loss rate and velocity of disc winds. The resulting scaling relations will allow a better understanding of line-driving in general and also give some tools to estimate disc wind properties for many astrophysical applications before calculating detailed multidimensional time-dependent numerical models.

We describe our numerical calculations in Section 2, present and compare our results in Section 3, and conclude with a discussion in Section 4. The Appendix summarizes the analytic results for \dot{M} and the velocity law in the CAK framework.

2 NUMERICAL METHODS

To calculate wind models we adopt the 2.5-dimensional hydrodynamical numerical method described by DPS (see also PSD). These models incorporate a non-rotating star, and a geometrically-thin and optically-thick accretion disc. The star and disc can both be a source of radiation and mass. PSD's formalism allows the stellar radiation to be included both as a direct contributor to the radiation force and as an indirect component via disc irradiation and re-emission. Each point on the disc and star is assumed to emit isotropically. The model takes into account stellar gravity, gas pressure effects, and rotational and radiation forces. The gas in the wind is taken to be isothermal. In the dimensional form of the equations of motion for the wind model studied by PSD there are six model parameters: the stellar Eddington number, $\Gamma_* = \frac{L_* \sigma_e}{4\pi c G M_*}$, the disc Eddington number, $\Gamma_D = \frac{L_D \sigma_e}{4\pi c G M_*}$, ($\Gamma_* = x \Gamma_D$ using the PSD x parameter; all other symbols have their conventional meaning), the normalised sound speed, c'_s , and three parameters describing the force multiplier, α , k and η_{max} (see Appendix). For parameters suitable for CVs (see PSD's table 1) the unit time, $\tau = \sqrt{r_*^3 / (G M_*)} = 2.88s$, the unit

and mass-loss rate. Their approach was to assume that the radiation force is abruptly cut off at an adjustable distance from the star.

velocity $v_0 = \sqrt{GM_*/r_*} = 3017 \text{ km s}^{-1}$, the unit mass-loss rate, $\dot{M}_0 = 8\pi cr_*/\sigma_e = 2.62 \times 10^{-5} M_\odot \text{ yr}^{-1}$ and $c'_s = c_s/v_0 = 4.6 \times 10^{-3}$.

Our calculations for stellar winds are as described in DPS with some changes outlined below. Because of the assumed spherical symmetry for stellar winds we use spherically symmetric initial and boundary conditions. We set all initial velocity components to zero, except the radial component, v_r , for which we use the CAK velocity (see equations A12 and A13). The density profile is given by hydrostatic equilibrium in the subsonic region and the CAK density profile (i.e., using the continuity equation, the CAK velocity law and mass-loss rate) in the supersonic region. The wind base density, ρ_{lb} , was chosen to sample the subsonic part of the flow and to allow initial transients to disappear on a short timescale. Typically, we use $\rho_{lb} = 10^{-10} \text{ g cm}^{-3}$. The radiation force is recalculated using the method described in PSD for the case without a disc. Here we would like to mention that in PSD, DPS and Oudmaijer et al. (1998) the radiation force due to lines from a star was calculated using equation (A5), not PSD's equation (C2). Thus all previous calculations of those authors were with a finite disc correction.

To confirm and extend the PSD results, we present some additional disc models with $\alpha = 0.4, 0.6$ and 0.8 calculated for various disc luminosities and with the stellar radiation switched off. The disc wind models are calculated as described in PSD.

In numerical calculations with a finite line-force cut-off we used two approaches to saturate the force multiplier. The first approach we considered is simply:

$$M(t) = \begin{cases} kt^{-\alpha} & \text{for } t > t_{min} \\ M_{max} & \text{for } t \leq t_{min} \end{cases} \quad (1)$$

where t_{min} is chosen so $kt_{min}^{-\alpha} = M_{max}$.

Our second, more physical approach, is that $M(t)$ saturates gradually as the wind material becomes more optically thin (see also PSD). Specifically, we follow OCR who introduced an exponential cutoff in the line distribution which ensures the force multiplier saturates smoothly:

$$M(t) = kt^{-\alpha} \left[\frac{(1 + \tau_{max})^{(1-\alpha)} - 1}{\tau_{max}^{(1-\alpha)}} \right] \quad (2)$$

where $\tau_{max} = t\eta_{max}$ and η_{max} is a parameter related to the most optically thick lines. Equation (2) shows the following limiting behaviour:

$$\lim_{\tau_{max} \rightarrow \infty} M(t) = kt^{-\alpha} \quad (3)$$

$$\lim_{\tau_{max} \rightarrow 0} M(t) = M_{max,e} = k(1-\alpha)\eta_{max}^\alpha. \quad (4)$$

For stellar winds, we calculated a few numerical test models to compare with analytic results summarized in the Appendix. We found good agreement between the numerical and analytic results - typically better than a few per cent.

3 RESULTS

Table 1 lists the parameter ranges explored in our numerical simulations. Generally, Γ_* and Γ_D control all the other parameters because they determine the wind photoionization structure for a given chemical composition. We thus need to explore only Γ_* and Γ_D provided we calculate self-consistently the wind photoionization structure and subsequently the radiation force. Unfortunately, this is not feasible due to the wind's multidimensional nature and its potential time variability. However using models calculated for stellar winds and some basic physical arguments we may consider coupling between α , η_{max} , and k without detailed photoionization calculations. Specifically, we are guided in this matter by the results showed by Abbott (1982) and Stevens & Kallman (1990) and references therein.

Using results of previous radiative force calculations for single stars and arguments from atomic physics, Gayley (1995) argues that the maximum force multiplier, M_{max} is relatively constant and depends on metallicity only. Gayley found that $M_{max} \sim$ a few 10^3 . Stevens & Kallman (1990) calculated the radiative force for a stellar wind ionized by an external X-ray source in massive X-ray binary systems. Their predicted maximum force multiplier is also a few 10^3 and is nearly constant for low ionization parameter. For a very high photoionization parameter, M_{max} decreases to zero as all ions in a wind lose all electrons and there is a reducing contribution to the radiation pressure from lines. Stevens & Kallman showed how the force multiplier decreases with the photoionization parameter. We will return to this point in Section 4.

Table 2 summarizes our numerical results for stellar winds while Table 3 summarizes PSD's results and ours for disc winds with $\Gamma_* = 0$.

3.1 Dependence of wind properties on Γ and M_{max}

Previous models of stellar winds driven by radiation force have explored a wide range of model parameters suitable for hot luminous stars. In the Appendix we briefly describe the basics of the CAK method, with the finite disc correction (hereafter CAK&FD), and with explicit introduction of M_{max} (hereafter CAK,FD& M_{max}). We also summarize the analytic results for \dot{M}_* and the velocity law.

In Fig. 1 we show (a) model mass-loss rates and (b) the terminal/typical velocities as functions of the Eddington number. All models on Fig. 1 are for $\alpha = 0.6$, $k =$

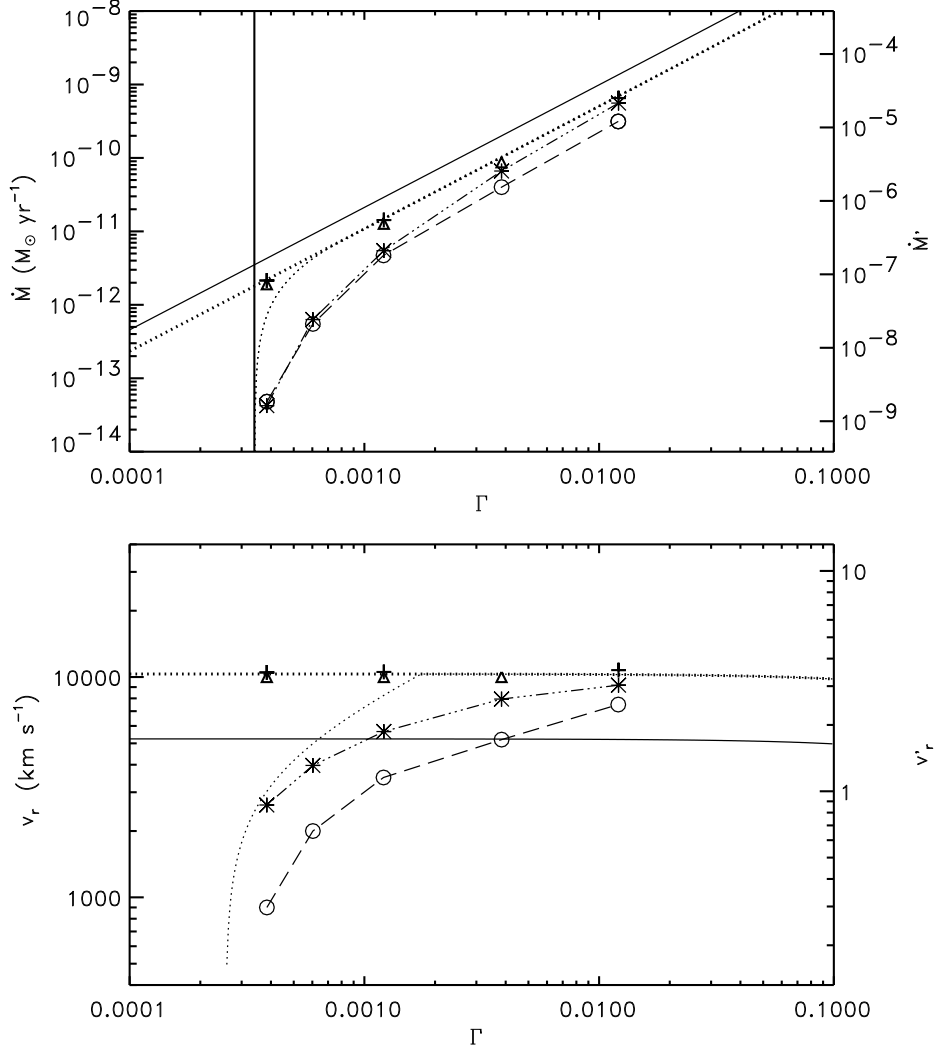


Figure 1. Model mass-loss rates (upper panel) and terminal/typical velocities (lower panel) as functions of the Eddington number. The solid lines plot results for stellar models in the CAK case (equations A13 and A14), while the thin dotted lines plot results for stellar models in the *CAK, FD&M_{max}* case (equations A25 and A26). The thick dotted lines plot results for stellar models in the *CAK&FD* case (equations A18, A19, and A20) while the crosses correspond to numerical results in this case. The asterisks connected by the triple-dot dashed lines correspond to numerical results for stellar models in the *CAK, FD&M_{max,e}* case. The open triangles represent disc results for models in the *CAK, FD&M_{max,e}* case while the open circles, connected by the dashed lines, represent disc results in the *CAK, FD&M_{max,e}* case. On upper panel the thick solid vertical line is for $\Gamma = 1/(1 + M_{max} f_{FD,c})$. The alternative ordinate on the right hand side of the upper panel is the dimensionless wind mass-loss rate parameter, $\dot{M}' = \dot{M}/\dot{M}_0$, and on the lower panel it is the dimensionless velocity parameter, $v_r' = v_r/v_0$.

0.2 and $M_{max} = 4400$. We plot analytic results for the stellar mass-loss rate, \dot{M}_* , and the terminal velocity, v_∞ in four cases: *CAK*, *CAK&FD*, *CAK, FD&M_{max}*, and *CAK, FD&M_{max,e}*. The last case, *CAK, FD&M_{max,e}* is where the finite disc factor and OCR's exponential cutoff in the line distribution are included.

For high Γ_* , the results shown on Fig. 1(a) confirm the well known CAK relation $\dot{M}_* \propto \Gamma_*^{1/\alpha}$ (the thin solid and thick dotted lines). Additionally our results confirm that the inclusion of the finite disc correction reduces \dot{M}_* by a factor of $\sim 2 \approx (1 + \alpha)^{1/\alpha}$, for $\alpha \sim 0.6$ (Friend & Abbott 1986 and PPK). This figure also reveals that the CAK scaling does not apply for very small Γ_* if we take into account the fact

that the force multiplier can not increase to arbitrarily high value (the thin dotted line and the asterisks). Our analysis presented in Appendix shows that the CAK scaling does not apply for

$$\Gamma_* \leq 1/(1 + (1 - \alpha) f_{FD,c} M_{max}). \quad (5)$$

The mass loss vanishes at

$$\Gamma_* = 1/(1 + M_{max} f_{FD,c}). \quad (6)$$

Previous studies by other authors of line driven stel-

Table 2. Summary of numerical results for stellar winds with $\alpha = 0.6$, $k=0.2$ and $M_{max} = 4400$.

Γ_*	\dot{M}_* ($M_\odot \text{ yr}^{-1}$)	$v_r(10r_*)$ (km s^{-1})
<i>CAK, FD&M_{max}</i> case		
3.84×10^{-4}	9.0×10^{-13}	2770
6.03×10^{-4}	4.1×10^{-12}	4550
1.21×10^{-3}	1.4×10^{-11}	7640
3.84×10^{-3}	9.6×10^{-11}	11130
1.21×10^{-2}	6.5×10^{-10}	10750
<i>CAK, FD&M_{max,e}</i> case		
3.84×10^{-4}	4.2×10^{-14}	2630
6.03×10^{-4}	6.3×10^{-13}	3970
1.21×10^{-3}	5.5×10^{-12}	5660
3.84×10^{-3}	6.6×10^{-11}	7940
1.21×10^{-2}	5.6×10^{-10}	9180

lar winds were for luminous stars for which the presence of M_{max} was not important. However for $\Gamma_* \lesssim 0.01$ in the *CAK, FD&M_{max}* case, \dot{M}_* is lower and the \dot{M}_* vs. Γ_* relation is steeper than in the *CAK&FD* case. For $\Gamma_* > 0.01$, \dot{M}_* in the *CAK, FD&M_{max}* case converges with \dot{M}_* in the *CAK&FD* case. On the other hand, \dot{M}_* in the *CAK, FD&M_{max,e}* case is steeper than in the *CAK, FD&M_{max}* case. Additionally, \dot{M}_* in the *CAK, FD&M_{max,e}* case converges with \dot{M}_* in the *CAK&FD* case for higher Γ_* than with \dot{M}_* in the *CAK, FD&M_{max}* case.

Fig. 1(a) also shows numerical results for the disc mass-loss rate, \dot{M}_D , from PSD (with a new point for $\Gamma_D = 6.03 \times 10^{-4}$, see Table 3), and for disc wind models with infinite M_{max} , the open circles and triangles, respectively. PSD results are analogous to stellar results in the *CAK, FD&M_{max,e}* case, while disc results with infinite M_{max} are analogous to stellar results for the *CAK, FD* case. Comparison between these analogue models demonstrates that the stellar mass-loss rate and the disc mass-loss rate depend on luminosity in a similar way for all luminosities. The most convincing case is for disc wind models with infinite M_{max} where disc mass-loss rate predictions almost match the results for the stellar *CAK&FD* case. In the *CAK, FD&M_{max,e}* case, lower \dot{M}_D approaches \dot{M}_* in the stellar *CAK, FD&M_{max}* and *CAK&FD* cases as the Eddington number increases.

Fig. 1(b) illustrates the behavior of v_∞ with the Eddington number. The CAK theory predicts that v_∞ stays almost constant with Γ_* for $\Gamma_* \ll 1$ (see equation A13). Friend & Abbott (1986) showed that the finite disc factor introduces a dependence of v_∞ on Γ_* but it is a weak dependence. Our calculations confirm these results and also confirm that v_∞ is higher for the *CAK&FD* case than for the *CAK* case by a factor of ~ 2 (Friend & Abbott 1986; PPK). However if we take into account M_{max} , v_∞ decreases strongly with decreasing Γ_* (see also equation A22).

Comparing results shown in Fig. 1, we find that for the *CAK, FD&M_{max}* case v_∞ remains sensitive to M_{max} for higher Γ_* than \dot{M}_* . Quantitatively v_∞ in the *CAK, FD&M_{max}* case starts to deviate from v_∞ in the *CAK&FD* case at

$$\Gamma_* = 1/(1 + 2(1 - \alpha)f_{FD,c}M_{max})$$

while \dot{M}_* starts to deviate at

$$\Gamma_* = 1/(1 + (1 - \alpha)f_{FD,c}M_{max}),$$

higher than the former by a factor of ≈ 2 . This is unsurprising, given that the terminal velocity of stellar winds is a global quantity determined in the whole acceleration zone whereas \dot{M} is a local quantity determined at the critical point and conserved in steady state models (see also Abbott & Friend 1989).

The characteristic velocity of disk winds does not depend on the Eddington number for infinite M_{max} . However for $M_{max} = 4400$, the characteristic velocity is a strong function of Γ_D . Thus the disk wind velocity and the stellar wind velocity are sensitive to the Eddington number in similar ways. The main difference is that disc winds react to finite M_{max} for higher Eddington number than stellar winds. This difference indicates that $M(t_c)$ is higher for discs than for stars.

So far we showed that a finite M_{max} reduces \dot{M}_* and v_∞ significantly unless $M(t_c) < M_{max}$. In the regime where $M(t_c) < M_{max}$ the actual value of M_{max} does not matter and \dot{M}_* and v_∞ do not depend on M_{max} nor η_{max} . As CAK found the main stellar properties are determined at the wind critical point. For example, equation (A18) shows how the mass-loss rate depends on the force multiplier at the criti-

Table 3. Summary of parameter survey for disc winds with $k = 0.2$ and $M_{max} = 4400$.

α	Γ_D	\dot{M}_D ($M_\odot \text{ yr}^{-1}$)	$v_r(10r_*)$ (km s^{-1})	run number in PSD
<i>CAK, FD case</i>				
0.6	3.84×10^{-4}	1.9×10^{-12}	10000	
0.6	1.21×10^{-3}	1.3×10^{-11}	10000	
0.6	3.84×10^{-3}	8.7×10^{-11}	10000	
<i>CAK, FD&$M_{max,e}$ case</i>				
0.4	3.84×10^{-4}	2.0×10^{-17}	700	
0.4	6.03×10^{-4}	6.3×10^{-16}	1400	
0.4	1.21×10^{-3}	6.3×10^{-15}	3000	15
0.4	3.84×10^{-3}	1.6×10^{-13}	6000	16
0.4	1.21×10^{-2}	2.4×10^{-12}	10000	
0.6	3.84×10^{-4}	4.8×10^{-14}	900	2
0.6	6.03×10^{-4}	5.5×10^{-13}	2000	
0.6	1.21×10^{-3}	4.7×10^{-12}	3500	3
0.6	3.84×10^{-3}	4.0×10^{-11}	5200 ^(a)	4
0.6	1.21×10^{-2}	3.1×10^{-10}	7500	5
0.8	3.84×10^{-4}	1.9×10^{-13}	500	
0.8	6.03×10^{-4}	8.8×10^{-12}	1200	
0.8	1.21×10^{-3}	6.2×10^{-11}	2500	17
0.8	3.84×10^{-3}	6.3×10^{-10}	7500	18
0.8	1.21×10^{-2}	4.0×10^{-9}	14000	19

a) We re-estimated a typical velocity for this model.

cal point. We can also express wind terminal velocity as a function of $M(t_c)$:

$$v_\infty^2 \propto \frac{(1 - \Gamma_*)}{(1 - \alpha)} = M(t_c)\Gamma_* \quad (7)$$

(see the Appendix). Thus luminous stars do not use all their available effective radiative force to drive winds. However for low luminosity stars, the importance of M_{max} and the effective luminosity is essential as M_{max} limits $M(t_c)$. For example, equation (A22) shows that in a first order approximation $v_\infty^2 \propto M_{max}\Gamma_*$ (see equation 7). Physically, it means that if the force multiplier is saturated the radiation pressure accelerates the wind maximally which is proportional to $M_{max}\Gamma_*$, in the single-scattering limit. Additionally, as we showed in Fig. 1 for the stellar case and PSD showed for the disc case, radiation pressure cannot drive a wind if $M_{max}\Gamma < 1/f_{FD,c} \lesssim 1.6$, that is if the effective luminosity is less than the Eddington luminosity.

To confirm further that disc winds behave in the same way as stellar winds we calculated a test model to compare with PSD's fiducial steady model for $\Gamma_* = \Gamma_D = 1.21 \times 10^{-3}$ (their model 8). For the test model all parameters are as for the fiducial model except for $\Gamma_D = \Gamma_* = 3.84 \times 10^{-3}$, increased by a factor of $10/\pi$, and $M_{max} = 1380$ decreased by the same factor. With these parameters our test model has

$M_{max}\Gamma$ the same as the fiducial model and the Eddington numbers as PSD's model 9.

The results of our test model confirm expectations: the test model has \dot{M} as PSD's model 9 with the same Γ and $v_r(r_o)$ as PSD's model 8[†] with the same ΓM_{max} . The test model also settles into a steady state. Then the disk mass-loss rate, as the stellar mass-loss rate, depends on the Eddington number while velocity depends on the effective luminosity at the critical point.

3.2 Dependence of wind properties on α and k

In the stellar case for $M(t_c) < M_{max}$, the analytic solutions provide scaling of the wind properties on all model parameters. For example, the α parameter determines a slope of the power-law dependence of \dot{M}_* on luminosity and on k (i.e., $\dot{M}_* \propto (k\Gamma_*)^{1/\alpha}$).

For $M(t_c) > M_{max}$ in the *CAK, FD& M_{max}* case, α and k determine the slope of a *linear* dependence of \dot{M}_* on

[†] Note a typo in PSD's table 2: for model 8, \dot{M}_D should be $2.1 \times 10^{-15} M_\odot \text{ yr}^{-1}$ instead of $1.2 \times 10^{-15} M_\odot \text{ yr}^{-1}$.

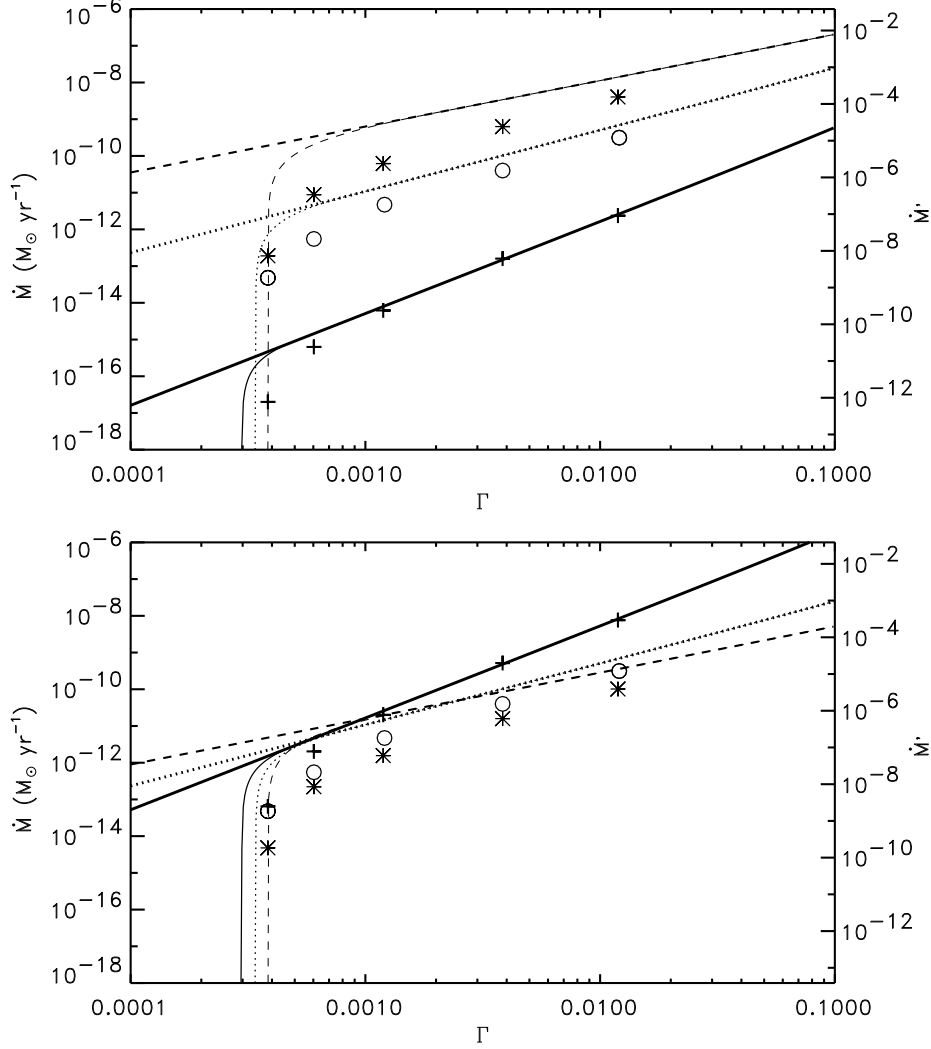


Figure 2. Model mass-loss rates as function of the Eddington number for $k = 0.2$ (upper panel) and k rescaled with α as described in Section 3.2 (lower panel). The thick lines represents results in the stellar *CAK&FD* case for $\alpha = 0.4, 0.6$ and 0.8 ; the solid, dotted, and dashed lines, respectively. The thin lines represents results in the stellar *CAK, FD& M_{max}* case, the line types are as in the *CAK&FD* case. The open circles represent results for the disc *CAK, FD& $M_{max,e}$* case and $\alpha = 0.6$, while the crosses and asterisks represent results for $\alpha = 0.4$ and $\alpha = 0.8$, respectively. The alternative ordinate on the right hand side of the two panels is as in Fig. 1(a).

luminosity: $\dot{M}_* \propto \Gamma k^{1/\alpha}$. Additionally, α enters the expression for $M(t_c)$ and then determines the lowest value of Γ for which $M(t_c) < M_{max}$ and the power-law applies (see equation 5). Moreover, through $f_{FD,c}$ the α parameter defines the lower limit of Γ for which a wind solution exists (see equation 6).

Fig. 2 illustrates how the mass-loss rate depends on the Eddington number for various α with (a) $k = 0.2$ and (b) k rescaled with α (see below). Fig. 2 also compares our predictions for \dot{M}_* and \dot{M}_D . We do not consider the *CAK, FD, & M_{max}* case with $\alpha = 0.4$ and 0.8 because our calculations for $\alpha = 0.6$ are sufficient to show the basic behavior in this case.

In the disc case, we used PSD's results complemented by our results. PSD calculated a few disc wind models with $\alpha = 0.4, 0.6$ and 0.8 for various disc and stellar luminosities

in the *CAK, FD& $M_{max,e}$* case. They found that there is no change in the power-law dependence of \dot{M}_D on luminosity between $\alpha = 0.6$ and $\alpha = 0.8$, in contrast to scaling found for the stellar wind solutions.

The analysis in previous subsection showed that \dot{M}_D scales with the Eddington number for $\alpha = 0.6$ almost as \dot{M}_* . However the analysis also showed that the *CAK* scaling does not apply in both the disc and stellar cases if Γ is very low and a finite M_{max} is used. Using these conclusions about similarities between disc and stellar winds, a simple interpretation of the PSD results for $\alpha = 0.8$ is that for these disc models $M(t_c) < M_{max}$ and the power-law does not apply. As we mentioned above, $M(t_c)$ increases with α (equation A17) and subsequently the lowest Γ for which the power-law applies, increases to unity with α , (equation 1). Then for a fairly high $\alpha = 0.8$, even the highest-considered Γ in Fig. 2 might still be in the region where the power-law

does not apply in the disc *CAK, FD&M_{max,e}* case. If so, no change in the power-law found by PSD and confirmed here can be seen as cancellation of the two opposite trends 1) a decrease of the slope caused by higher α and 2) an increase of the slope caused by a finite M_{max} (see Fig. 1).

This interpretation is confirmed by the results for disc winds with $\alpha = 0.4$. Fig. 2 shows that for $\alpha = 0.4$, the slope is as predicted by the *CAK&FD* scaling and the power-law applies for a Eddington number range wider than for $\alpha = 0.6$ and $\alpha = 0.8$.

In their preliminary parameter survey, PSD calculated disc wind models for different α and Γ_D while holding M_{max} and k fixed. In their formalism, they did that by means of adjusting a value of η_{max} according to the equation

$$\eta_{max} = \left(\frac{M_{max}}{k(1-\alpha)} \right)^{1/\alpha}. \quad (8)$$

As we mentioned in Section 3.1 Gayley (1995) showed that M_{max} can be interpreted as a pseudo-conserved quantity that is proportional to metallicity and is estimable a priori. However k depends on metallicity, sound speed and the other force multiplier parameters (e.g., *CAK*, Gayley 1995). Assuming that M_{max} is constant and using equation (4) we can express k as

$$k = \frac{1}{1-\alpha} \eta_{max}^{-\alpha} M_{max}. \quad (9)$$

Additionally adopting Gayley's working assumption that we truncate the line distribution at the single strongest line (i.e., $M_{max} = \frac{v_{th}}{c} \eta_{max}$ using our notation) we can rewrite equation (9) as

$$k = \frac{1}{1-\alpha} \left(\frac{v_{th}}{c} \right)^\alpha M_{max}^{1-\alpha}. \quad (10)$$

The last equation shows explicitly how the formal parameter k depends on physical properties of wind.

In this context we could ask how PSD's and our results for fixed k and M_{max} can be rescaled to accommodate the coupling of k with other model parameters.

Using the result for stellar winds: $\dot{M} \propto k^{1/\alpha}$, we can rescale the mass-loss rates for a new k parameter, k_n if we multiply \dot{M} by the correction factor:

$$f_k = \left(\frac{k_n}{k} \right)^{1/\alpha}. \quad (11)$$

The detailed calculations of the force multiplier and stellar winds (e.g., *CAK*; Abbott 1982; Gayley 1995) showed

that the mass-loss rate increases with decreasing α . This result can be understood if we consider the coupling between the parameters of the force multiplier. As equation (9) shows, k increases with decreasing α causing an overall increase of $M(t)$ and subsequently an increase of \dot{M} .

PSD's results suggest that \dot{M}_* increases with α . This result is the consequence of changing α but formally keeping k constant. We found a similar behaviour of \dot{M}_* (see Fig. 2a) when we applied PSD's approach. However our previous analysis and numerical tests show that we can rescale \dot{M}_D if other k is chosen. For example, if we take PSD models for $\alpha = 0.4$ and 0.8 and want to rescale them, keeping M_{max} and η_{max} as for $\alpha = 0.6$ (i.e., $M_{max} = 4400$ and $\eta_{max} = 10^{7.9}$) we need first calculate k_n using equation (9) and then use the correction factor f_k . In the example considered here the correction factor is:

$$f_k = \left(\frac{4400}{0.2(1-\alpha)} \right)^{1/\alpha} 10^{-7.9}. \quad (12)$$

Fig. 2b shows results from Fig. 2a, where the mass-loss rates for $\alpha = 0.4$ and 0.8 are rescaled as described. The results for $\alpha = 0.6$ are unchanged. Fig. 2a clearly shows that after rescaling \dot{M}_D and \dot{M}_* increase with decreasing α as found in previous stellar wind models.

Contrary to the mass-loss rate, the terminal velocity does not depend on k (e.g., equations A13, A22, and A25). Our numerical tests confirm this for stellar and disk winds.

3.3 Dependence of wind properties on sound speed

Analytic steady state solutions of stellar winds depend very weakly on the sound speed (e.g., *CAK*; *PPK*). Numerical simulations of stellar winds showed that a higher c_s shortens the computational time needed for the initial conditions to settle into a steady state (e.g., *OCR*). However the final steady state solution does not depend on c_s . Our numerical tests confirm these results for stellar winds. We thus do not expect changes of our disc wind results with c_s either. Nevertheless we calculated a few models for various c_s .

We have calculated models with c'_s higher and lower than $c'_s = 4.6 \times 10^{-3}$ by a factor of 3 and compare them with PSD's fiducial complex and steady models, PSD's model 2 and 8 respectively. We found that \dot{M}_D and velocity of the disc winds do not depend on c'_s . However, the time behaviour of the winds does depend. For example, the PSD fiducial steady state model recalculated with $c'_s = 1.53 \times 10^{-3}$ is somewhat time dependent: density fluctuations originating in the wind base spread in the form of streams sweeping outward. We did not find infalls of dense clumps of gas on the disc. On the other hand, the model as the PSD fiducial complex model but with $c'_s = 1.38 \times 10^{-2}$ settles into much

smoother and steadier state than PSD's model 2. Generally, we found that wind time dependence weakens with increasing c'_s because the gas pressure effects get stronger with increasing c'_s . Subsequently higher gas pressure smooths the flow more effectively and in a larger region above the disc mid-plane as the size of the subcritical part of the flow increases with c'_s .

4 DISCUSSION

Our comparison between disc and stellar winds has shown that despite differences in geometry, these two winds are similar in terms of \dot{M} and v_∞ . In particular, we showed that \dot{M}_* is an upper limit on \dot{M}_D for the same model parameters, typically $\dot{M}_*/\dot{M}_D \lesssim 2$.

Previous CV wind simulations showed that the predicted \dot{M}_D is lower than the observed \dot{M}_D by a factor of a few, at best (e.g., Drew 1997, PSD and references therein). If we use \dot{M}_* for the Eddington number and other model parameters as for CV's accretion discs we still may not reproduce observed disc mass-loss rates. Thus we might conclude that 1) present disc wind models still need some important improvement or 2) \dot{M}_D inferred from observations are over-estimated, or both. At the moment redetermination of \dot{M}_D from observations taking into account wind structure predicted by PSD is probably better than moving directly to exploring different ways of enhancing theoretical \dot{M}_D (e.g., including magnetic field effects). Such an approach will provide better constraints on our disk wind model.

Our tests with different sound speeds showed that thermodynamic effects might be important in determining time behavior of the disc winds. However we do not believe that a sound speed higher by a factor of 3 compared to the one used PSD for CVs is possible because this could correspond to the wind temperature higher by a factor of 9! Thus we do not expect great changes in models for CV disc winds after the inclusion of temperature calculations.

Thermodynamics and changes in wind photoionization might be important in very luminous systems such as AGNs and X-ray binaries. In studies of the former there is the long standing problem of wind over-ionization by the central radiation, especially in the inner part of an outflow. Such over-ionization will manifest in a low M_{max} , for instance. However it is arguable how damaging for radiation driving that can be. Using fiducial values for AGN's: $\Gamma = 0.4$ and $\alpha = 0.6$ (e.g., Murray et al. 1995; Arav 1996) and equation (A19), $M(t_c) = 3.75$. Our analysis showed that line driven winds are strong and fast when $M_{max} > M(t_c)$. Thus for AGNs to produce strong and fast line-driven winds not too many absorption lines are needed. Stevens & Kallman (1990) showed that $M_{max} < 4$ for relatively high photoionization parameters (see also Arav, Li & Begelman 1994; Murray et al. 1995). This simple argument supports the idea that winds in AGNs are line-driven.

To conclude we would like to mention that previous attempts to model disc winds using 1D approximations, have found some vindication in our fully 2D time-dependent simulations. This is not surprising, because of the energy argument: in both the stellar and disc cases most of the radiation energy is released near the central object. Thus the fully 2D calculations are crucial to determine the density and velocity as function of the position and time but less necessary to estimate the mass-loss rate and typical velocity for disc winds.

Acknowledgments: We would like to thank Janet Drew and James Stone for helpful discussions. Scott Kenyon is thanked for his comments and careful reading of the manuscript. This research has been supported by a research grant from PPARC. Computations were performed at the Pittsburgh Supercomputing Center and Imperial College Parallel Computing Centre.

APPENDIX A: SUMMARY OF ANALYTIC RESULTS FOR THE CAK MODEL WITH THE FINITE DISC CORRECTION AND A FINITE MAXIMUM FORCE MULTIPLIER.

The radial radiation force (per unit mass) due to spectral lines at every location in the flow can be expressed as

$$F^{rad,l} = \int \left(\frac{\sigma_e d\mathcal{F}}{c} \right) M(t), \quad (\text{A1})$$

where the term in brackets is the radiation force due to electron scattering from a stellar surface element and $d\mathcal{F}_*$ is the frequency integrated flux from that element. The integration is over the visible radiant surface. The quantity M , called the force multiplier, represents the increase in radiation force over the pure electron scattering case when lines are included. CAK found a fit to their numerical results for the force multiplier, such that

$$M(t) = kt^{-\alpha}, \quad (\text{A2})$$

where k and α are parameters of the fit. In the Sobolev approximation, $M(t)$ is a function of the optical depth parameter

$$t = \sigma_e \rho v_{th} \left| \frac{dv_l}{dl} \right|^{-1}, \quad (\text{A3})$$

where ρ is the density, v_{th} is the thermal velocity, and $\frac{dv_l}{dl}$ is the velocity gradient along the direction linking a point in the wind to the radiant surface element. For a spherically-expanding wind,

$$\frac{dv_l}{dl} = \frac{dv_r}{dr} \mu^2 + \frac{v_r}{r} (1 - \mu^2), \quad (\text{A4})$$

where v_r is the radial wind velocity and μ is the direction cosine.

Making an assumption $\frac{dv_r}{dr} \gg \frac{v_r}{r}$, certainly valid in a lower part of the wind acceleration zone, $\frac{dv_l}{dl}$ is

$$\frac{dv_l}{dl} = \frac{dv_r}{dr} \mu^2. \quad (\text{A5})$$

Then using equations (A3) and (A4), the equation for $F^{rad,l}$ is

$$F^{rad,l} = \left(\frac{\sigma_e \mathcal{F}_*}{c} \right) f_{FD} M_{CAK}(t), \quad (\text{A6})$$

where \mathcal{F}_* is the frequency integrated flux from the star, $M_{CAK}(t) = k \left(\sigma_e \rho v_{th} \left| \frac{dv_r}{dr} \right|^{-1} \right)^{-\alpha}$, is the force multiplier in the form introduced by CAK, and f_{FD} is the so-called finite disc correction factor which allows a generalization of the CAK formalism beyond the point-star case. The assumption made above simplifies the finite disc factor to a function of radius only:

$$f_{FD}(r) = \frac{1 - (1 - r_*^2/r^2)^{\alpha+1}}{(1 + \alpha)r_*^2/r^2}. \quad (\text{A7})$$

Using the Eddington number, $\Gamma_* = \frac{L_* \sigma_e}{4\pi c G M_*}$, where all symbols have their conventional meaning, we can rewrite equation (A6) as

$$F^{rad,l} = \frac{GM\Gamma_*}{r^2} f_{FD}(r) kt^{-\alpha}. \quad (\text{A8})$$

The equation of motion for a spherical, steady state wind is

$$\left(v - \frac{c_s^2}{v}\right) \frac{dv}{dr} + \frac{GM_*(1 - \Gamma_*)}{r^2} + \frac{2c_s^2}{r} - \frac{dc_s^2}{dr} + F^{rad,l} = 0 \quad (\text{A9})$$

where c_s is the gas sound speed. We dropped the 'r' subscript for simplicity. The principles of solving this equation of motion are presented in CAK (see also PPK). Here we generally follow them to calculate the velocity law and the stellar mass-loss rate in the zero sound speed case. Equation (A9) reduces to

$$v \frac{dv}{dr} + \frac{GM_*(1 - \Gamma_*)}{r^2} + F^{rad,l} = 0. \quad (\text{A10})$$

Using the continuity equation and equation (A8), equation (A10) becomes:

$$vv' + \frac{GM_*(1 - \Gamma_*)}{r^2} + \frac{GM\Gamma_*}{r^2} f_{FD}(r) k \left(\frac{4\pi}{\sigma_e v_{th} \dot{M}_*}\right)^\alpha (vv')^\alpha = 0, \quad (\text{A11})$$

where $v' = \frac{dv}{dr}$.

Assuming $f_{FD}(r) = 1$, we have the case considered by CAK. Here we repeat their well known solutions for the velocity law

$$v(r) = v_\infty (1 - r_*/r)^\beta. \quad (\text{A12})$$

where $\beta = 0.5$,

$$v_\infty^2 = \frac{\alpha}{1 - \alpha} \left(\frac{2GM_*(1 - \Gamma_*)}{r_*}\right) \quad (\text{A13})$$

and the mass-loss rate

$$\dot{M}_* = \frac{4\pi GM_*}{\sigma_e v_{th}} \frac{\alpha}{1 - \alpha} (1 - \Gamma_*)^{-(1-\alpha)/\alpha} ((1 - \alpha)k\Gamma_*)^{1/\alpha}. \quad (\text{A14})$$

When the star is treated as a point-source, the optical depth parameter does not vary with radius and is

$$t = \frac{v_{th} \dot{M}_* \sigma_e}{2\pi v_\infty^2 r_*} \quad (\text{A15})$$

and subsequently

$$M(t) = k \left(\frac{v_{th} \dot{M}_* \sigma_e}{2\pi v_\infty^2 r_*}\right)^{-\alpha}. \quad (\text{A16})$$

On the other hand using the critical point conditions (see CAK, PPK and Gayley 1995) the force multiplier is

$$M(t) = M(t_c) = \frac{1 - \Gamma_*}{(1 - \alpha)\Gamma_*}, \quad (\text{A17})$$

where the 'c' subscript indicates that a quantity is evaluated at the wind critical point.

Comparing the right hand sides of equations (A16) and (A17) and using equation (A13), \dot{M}_* can be expressed as

$$\dot{M}_* = \frac{4\pi GM_*(1-\Gamma_*)}{\sigma_e v_{th}} \frac{\alpha}{1-\alpha} \left(\frac{k}{M(t_c)} \right)^{1/\alpha}. \quad (\text{A18})$$

Equation (A18) demonstrates the importance of the force multiplier at the critical point in determining the mass-loss rate.

For the finite disc case, the mass-loss rate is also given by equation (A18) but the force multiplier at the critical points is now

$$M(t_c) = \frac{1-\Gamma_*}{(1-\alpha)\Gamma_* f_{FD,c}}. \quad (\text{A19})$$

For the velocity law we assume that it can be approximated by equation (A12) and find that

$$v_\infty^2 = \frac{\alpha}{1-\alpha} \frac{GM_*(1-\Gamma_*)}{r_*} \frac{1}{\beta} (1-r_*/r_c)^{-2\beta+1}. \quad (\text{A20})$$

We confirm PPK results that this approximation works fairly well for $\beta = 0.8$ and $r_c = 1.05r_*$. Note that in this case the force multiplier increases with radius.

Now we move to a problem of solving the equation of motion when $M_{max} < M(t_c)$. In this case we assume that the force multiplier is constant, i.e., $M(t) = M_{max}$ for all locations in a wind. Such a simple approach allows the equation of motion to be written as

$$vv' + \frac{GM_*(1-\Gamma_*)}{r^2} + \frac{GM\Gamma_*}{r^2} f_{FD}(r) M_{max} = 0. \quad (\text{A21})$$

For $f_{FD} = 1$, we find that the velocity law is again as in the CAK case with

$$v_\infty^2 = \frac{2GM_*(\Gamma_*(1+M_{max})-1)}{r_*}, \quad (\text{A22})$$

while the mass-loss rate is

$$\dot{M}_* = \frac{4\pi GM_*(\Gamma_*(1+M_{max})-1)}{\sigma_e v_{th}} \left(\frac{k}{M_{max}} \right)^{1/\alpha}. \quad (\text{A23})$$

For the finite disc case, the velocity law is:

$$v(r) = \left(\frac{2GM}{(1+\alpha)rr_*^2} ((1+\alpha)(1-\Gamma_*)r_*^2 + \Gamma_* M_{max} (r^2(1-H2F1(-0.5, -\alpha; 0.5; \frac{r_*^2}{r^2}))) - r_*^2 H2F1(0.5, -\alpha; 1.5; \frac{r_*^2}{r^2})) + rr_*(\Gamma_*(1-M_{max}(1-h1-h2)) - \alpha(1-\Gamma_*) - 1) \right)^{1/2} \quad (\text{A24})$$

where H2F1 is hypergeometric function, $h1 = H2F1(-0.5, -\alpha; 0.5; 1)$ and $h2 = H2F1(0.5, -\alpha; 1.5; 1)$. The terminal velocity is

$$v_{\infty} = \left(\frac{2GM_*}{(1+\alpha)r_*} (\Gamma_*(1 - M_{max}(1 + \alpha/r_* - h_1 - h_2)) - \alpha(1 - \Gamma_*) - 1) \right)^{1/2}. \quad (\text{A25})$$

And finally the mass-loss rate is

$$\dot{M}_* = \frac{4\pi GM_*(\Gamma_*(1 + f_{FD,c}M_{max}) - 1)}{\sigma_e v_{th}} \left(\frac{k}{M_{max}} \right)^{1/\alpha}. \quad (\text{A26})$$

REFERENCES

- Abbott D.C. 1982, ApJ, 259, 282
 Abbott M.J., Friend D.B., 1989, ApJ, 345, 505
 Arav N., 1996, ApJ, 465, 617
 Arav N., Li Z.Y., Begelman M.C., 1994, ApJ, 432, 62
 Bjorkman J.E., Cassinelli J.P., 1993, ApJ, 409, 429
 Castor J.I., Abbott D.C., Klein R.I., 1975, ApJ, 195, 157 (CAK)
 Drew J.E., 1997, in Wickramasinghe D., Ferrario L., Bicknell G., eds, ASP Conf. Ser. 163, Accretion Phenomena and Related Outflows, Astron. Soc. Pac., San Francisco, p. 465
 Drew J.E., Proga D., Stone J.M., 1998, 296, L6 (DPS)
 Friend D.B., Abbott D.C., 1986, ApJ, 311, 701
 Gayley K.G., 1995, ApJ, 454, 410
 Icke V., 1980, AJ, 85, 329
 Icke V., 1981, ApJ, 247, 152
 Lucy L.B., Solomon P., 1970, ApJ, 159, 879
 Mundt R., Ray T.P., 1994, in *The nature and evolutionary status of Herbig Ae/Be stars*, eds. P.S. Thé, M. R. Pérez, E.P.J. van den Heuvel, ASP Conf.Sers. 62, 237
 Murray N., Chiang J., Grossman S.A. Voit, G.M., 1995, ApJ, 451, 498
 Oudmaijer R.D., Proga D., Drew J.E., de Winter D., 1998, MNRAS, 300, 170
 Owocki S.P., Cranmer S.R., Blondin J.M., 1994, ApJ, 424, 887
 Owocki S.P., Castor J.I., Rybicki, G.B., 1988, ApJ, 335, 914
 Pauldrach A., Puls J., Kudritzki R.P., 1986, A&A, 164, 86 (PPK)
 Pereyra N.A., Kallman T.R., Blondin J.M., 1997, ApJ, 477, 368
 Pereyra N.A., 1997. Ph.D. thesis, University of Maryland.
 Proga D., Stone J.M., Drew J.E., 1998, MNRAS, 295, 595 (PSD)
 Puls J., Owocki S.P., Fullerton A., 1993, A&A, 279, 457
 Stevens I.R., Kallman T.R., 1990, ApJ, 365, 321
 Vitello P.A.J., Shlosman I., 1988, ApJ, 327, 680
 Weymann R.J., Morris S.L., Foltz C.B., Hewett P.C., 1991, ApJ, 373, 23